

Computed Radiography Technology 2004

J. Anthony Seibert, Ph.D.

Department of Radiology
University of California Davis Medical Center
Sacramento, California

Introduction	154
The CR System	154
Image Acquisition	155
Point-Scan CR Readers	156
Line-Scan CR Readers	159
Image Data Pre-Processing	160
Shading Corrections	160
Identification and Scaling of “Pertinent” Data	161
Image Data Post-Processing	163
Contrast Enhancement	163
Spatial Frequency Enhancement	163
Multi-Scale, Multi-Frequency Enhancement	164
Disease-Specific and Dual-Energy Processing	165
The Physicist’s Role in CR Implementation	166
Clinical Considerations	166
CR Reader Throughput	166
Phosphor Plates, Cassettes, Grids, Identification Terminals	166
Incident Exposure Estimation and Other Data Fields	167
Image-Processing Functionality	167
CR Interfaces to RIS, HIS, Imaging Networks, and PACS	167
Quality Control Phantom Set and Software	168
Service Contracts, Preventive Maintenance, Warranty, and Siting Requirements	168
Exposure Indicators	168
Fuji CR: Sensitivity Number	168
Kodak CR: Exposure Index	169
Agfa CR: IgM Database	169
CR Exposure Recommendations	170
Spatial Resolution, Contrast Resolution, and Detective Quantum Efficiency (DQE)	171
Spatial Resolution	171
Contrast Resolution	172
Detective Quantum Efficiency (DQE)	173
CR Manufacturers	173
Conclusions	173
References	174

Introduction

Computed radiography (CR) technology has evolved over two decades of clinical use, beginning with the introduction of the Fuji FCR 101 in 1983. Since that time (and particularly in the 1990s), several manufacturers have realized the opportunities and the importance of CR clinical acquisition systems as necessary to the implementation of Picture Archiving and Communications Systems (PACS). These manufacturers have provided a wide range of capabilities—from large, high-throughput, multi-plate stackers to cassetteless and high-speed automated CR acquisition devices to small, desktop-sized, single-plate readers—to address the needs of the largest hospitals to the smallest outpatient clinics. A shift to an all-digital, filmless environment has also stimulated progress in the application of CR to pediatric and mammographic imaging and has brought added importance to image pre- and post-processing to take advantage of the flexibility provided by the digital format. This chapter addresses many technological changes occurring over the last decade. A brief review of the characteristics of photostimulated luminescence and the underlying physics of “computed” radiography image formation is followed by a description of the improvements and advances of photostimulable storage phosphor (PSP) detectors and how they compete with “direct” radiography devices in the clinical arena.

The CR System

A computed radiography device is composed of an independent, passive x-ray detector (a cassette-based PSP detector of various dimensions that is similar to conventional screen-film cassettes) and an image processor (also known as a CR “reader”), which processes the latent x-ray image captured by the detector. The PSP detector, which is commonly referred to as an imaging plate (IP), resides in a protective cassette. After latent image readout and digital signal conversion, the image data are accumulated, stored into a digital, two-dimensional (2-D) matrix, and transferred to a Quality Control (QC) review workstation. Patient demographic information is appended, and contrast/spatial frequency enhancement algorithms are applied to the digital image and/or adjusted before transfer to the PACS. Subsequent image viewing, diagnosis, and archiving are achieved outside of the direct interaction with the CR system, as illustrated in Figure 1. This process is notably similar to the 100-year-old screen-film paradigm, which is both a blessing and a curse. Blessings are in the form of positioning flexibility and the ubiquitous cassette form factor. The curse is in the extra handling and time required for processing the IP, which reduces workflow efficiency and patient throughput expected of a “digital” detector system. With that being said, CR systems are also designed as a cassetteless system that limits positioning but increases ease of use, which is similar to the advantages touted by “direct radiography” devices.

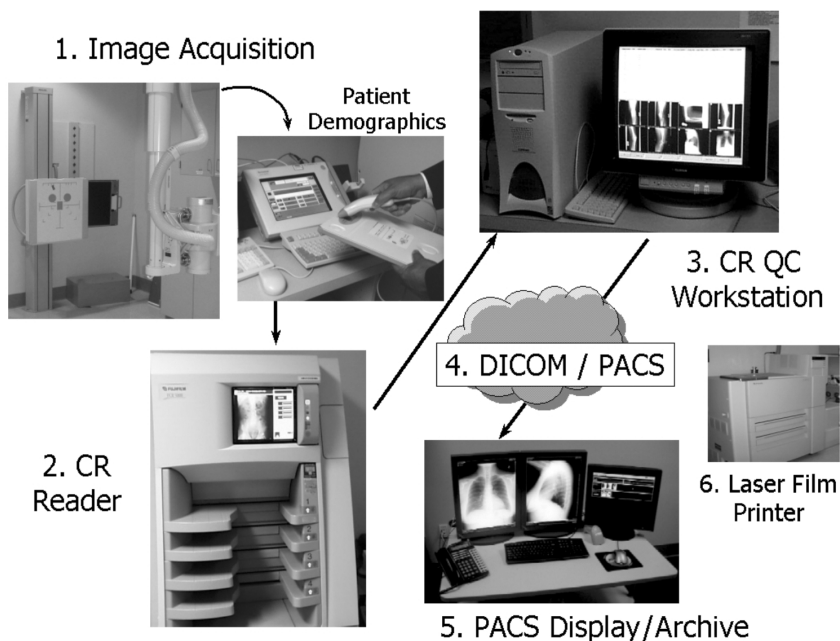


Figure 1. Representation of CR image acquisition and dataflow: 1. acquisition and identification; 2. processing; 3. quality control; 4. electronic transfer; 5. soft copy display and digital archiving; and 6. laser film printer (option).

Image Acquisition

The PSP material is a barium-fluoro-bromide/iodide (BaFBr/I) compound doped with trace amounts of europium (Eu). In operation, the PSP material captures transmitted x-ray flux and creates a transient latent image by the trapping of electrons from the ground state into spatially localized higher-energy-level “F-center” traps. X-rays absorbed in the phosphor create a proportional number of trapped electrons. The spatial distribution of trapped electrons represents the unprocessed latent image. X-ray absorption efficiency is dependent on energy of the x-ray photon and the thickness of the PSP compound and sets the upper limits of detective quantum efficiency (DQE) achievable with the CR imaging system. A relative comparison of BaFBr, Gd₂O₂S, and CsI is illustrated in Figure 2 for typical “standard” thicknesses used in radiographic detectors.

Extraction of the electron latent image requires a stimulating light source, which is usually a diode laser (680 nm wavelength), that pumps the electrons out of the trap to a higher energy level within the compound and then immediately to the ground state with only a short lag. As the electrons drop to the valence shell, emission of a blue, ~415 nm photostimulated luminescence (PSL) photon emerges from the

X-ray Absorption Efficiency: CsI, BaFBr, Gd₂O₂S

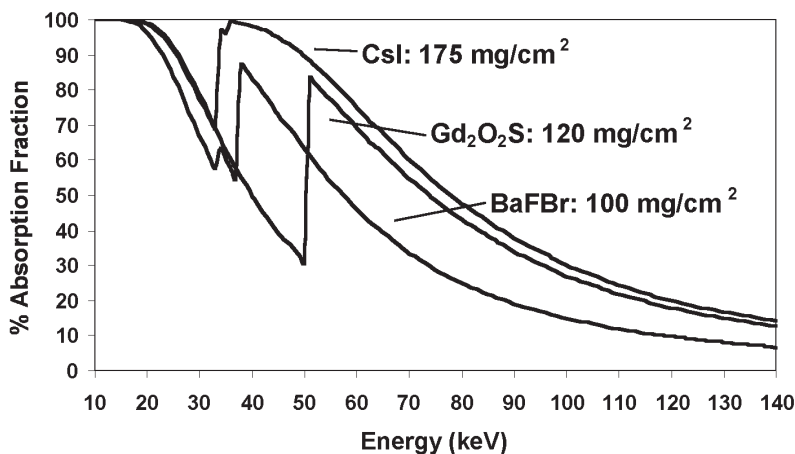


Figure 2. Absorption characteristics of BaFBr, CsI, and Gd₂O₂S phosphors of “typical” thickness for digital radiography. These characteristics are shown as a function of incident x-ray energy.

phosphor as the *visible* latent image signal (Takahashi et al. 1984; von Seggern et al. 1988). Because the PSL is of shorter wavelength than the stimulating source, optical filtering can separate these two “simultaneous” light sources. Collection and amplification of the signal with photosensitive electronic devices followed by digitization of the signal produces the equivalent digital signal. Spatial mapping of the output signals projected onto the detector is achieved by either point-scan methods using a small-diameter laser beam (e.g., 100 μm effective diameter) or the recently introduced laser beam line-scan methods discussed below.

Point-Scan CR Readers

The CR reader orchestrates the latent image extraction of the exposed IP and applies subsequent amplification and conversion to a digital signal. A typical reader is composed of an optical stage, scanning laser beam, IP translation mechanics, light pickup guide(s), photomultiplier tube (PMT), signal transformer/amplifier, and analog-to-digital converter (ADC). The exposed cassette is inserted into the reader, and the IP is extracted and translated through an optical stage by precisely controlled pinch rollers. As the plate is translated, the scanning laser beam sweeps across the plate row by row, with a speed that is adjusted according to the luminescent signal decay time constant ($\sim 0.8 \mu\text{s}$ for BaFBr:Eu²⁺). The effective laser beam spot size is controlled by the laser optics and f- θ lens, and the speed of IP translation is set to ensure appropriate coverage by the laser beam as well as to achieve equal sampling in the row and

column directions of the output digital image. The laser beam sweep is called the “scan” or “fast-scan” direction whereas the plate translation represents the “sub-scan” or “slow-scan” direction. This distinction is important for analyzing spatial resolution characteristics of the CR system and tracking down possible problems. An illustration of the CR reader components is shown in Figure 3. Readout of the detector typically requires from 45 to 90 seconds, depending on the specifications of the given CR reader (not including subsequent erasure of the residual signal so that the IP can be used again). Although the PSL is produced in all directions, only the light scattered backwards is collected. Recently introduced dual-side reading technology is now available, in which the phosphor material is layered on a transparent substrate and the forward-directed PSL is captured by a second light guide on the other side of the IP, thus increasing the capture efficiency of PSL. A thicker phosphor layer is also used, which increases the detective quantum efficiency of the system by up to 50% (Seibert, Boone, and Cooper 2002).

Spatial resolution depends on the laser beam spot size, the decay lag of PSL during the readout, the speed of the laser beam sweep, the frequency of the electronic sampling, and the translation speed of the IP. Because at any instant in time only a single point irradiates the IP, the capture of the PSL within the light guide will generate a signal that corresponds to that point. The spread of PSL within the light guide

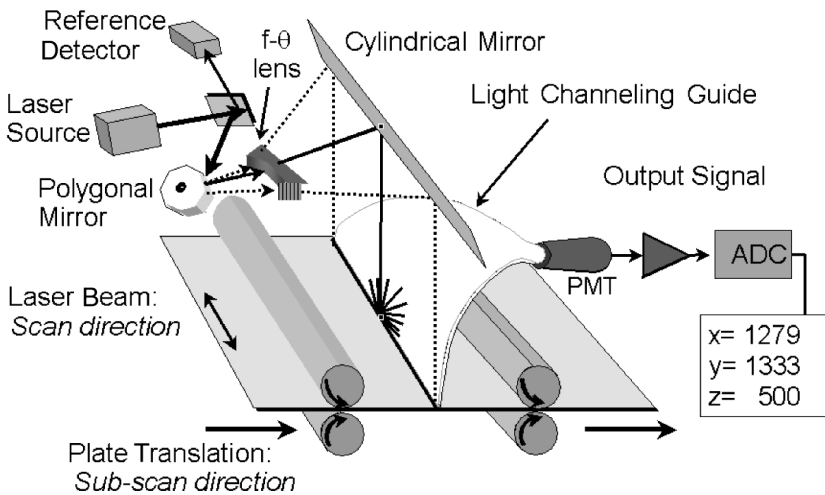


Figure 3. Internal components of a conventional point-scan CR reader. Components include the stimulating laser source, a beam splitter, oscillating beam deflector, $f-\theta$ lens, stationary reflecting mirror, light collection guide, photomultiplier tube (PMT), and ADC subsystem. The plate is translated in a continuous motion through the laser beam scan by pinch rollers.

In dual-side readout systems, a second light guide positioned underneath the scanning IP collects the PSL transmitted through the transparent substrate.

will not adversely affect resolution. (This is not, however, true of line-scan systems, described in the next section, which require a linear lens array to ensure proper mapping of the PSL generated from the IP to the source.) Adjustments are made to ensure that the resolution is approximately equal in the scan and sub-scan directions. Typical “effective” resolution element size is 100, 150, or 200 μm , which corresponds to 5.0 to 2.5 line pairs per millimeter (lp/mm)—certainly less than that achieved by a 400-speed screen-film system, which provides approximately 7.5 lp/mm.

Residual signals remain on the IP after readout; in fact, a given IP can be scanned several times and reveal a recognizable (albeit noisy) image. Thus, erasure is subsequently applied with the use of a high-intensity light source. In many systems, the length of erasure time is dependent on the x-ray exposure to the IP. Often, in severe overexposures (particularly for unattenuated beam areas), erasure can require several minutes to ensure adequate removal of the latent image and can be a potential bottleneck in sequential, single-plate reader systems. Verification of adequate erasure after a severe overexposure is one test to be performed at acceptance. These and other validations of performance are described in Seibert (2004) in this monograph. Another consideration is IP mechanical wear and tear, which can ultimately limit the lifetime of the detector. Systems that mechanically bend the IP during the readout will likely have a shorter lifetime and require earlier replacement than straight-through or solid plate IPs. A guarantee from the vendor on the number of cycle times is important for budgetary purposes because the combined IP and cassette costs are fairly substantial (\$1,000 or more, depending on contract prices, etc.), which significantly adds to the initial and ongoing upkeep/maintenance costs.

The PSL captured by the light guide(s) is optically filtered and channeled to the photocathode of the PMT(s), causing emission of electrons and subsequent acceleration and amplification through a series of dynodes. Overall gain of the PMT is controlled by the adjustment of the voltage placed on the dynodes, which is usually set at a fixed value that corresponds to the expected exposure levels for clinical diagnostic procedures. High gain and extremely large dynamic range of the PMT produces light intensity variations from the phosphor that span a range of 10,000, or “four orders of magnitude.” In older CR readers, a low-energy laser pre-scan was used to determine the range of x-ray exposures on the plate (and thus light emission) in order to adjust the gain of the PMT. Current readers use a preset PMT gain that achieves good linearity over clinical exposure ranges of usually 0.1 mR to 100 mR or 0.01 to 10 mR (determined by the preset gain of the PMT) to allow optimal digitization of the PSL signal intensities. Prior to conversion of the PMT signal to a digital value, most CR systems apply a non-linear transformation with a logarithmic or square-root amplifier. Logarithmic conversion provides a linear relationship of incident exposure to output signal amplitude; square-root amplification provides a linear relationship, with the noise associated with the exposure. In either case, the total dynamic range of signal is compressed so that digitization accuracy can be preserved over a limited number of discrete gray levels.

Line-Scan CR Readers

Fast, parallel CR line-scan systems are now available for clinical use; they are based on the simultaneous stimulation of the PSP *one line at a time* and the acquisition of the PSL with a charge-coupled-device (CCD) linear array photodetector (Arakawa et al. 2004). A scanning module contains several linear laser units, optical light collection lenses along the length of the scan unit, and an inline high-sensitivity CCD photosensitive array to capture the resultant PSL signal simultaneously, one row at a time (Figure 4). Unlike the point-scan system, which does not require focusing, the line-scan system has a lens array to focus the light along each point of the stimulated IP to a corresponding point on the CCD array. The module scans above the stationary IP of $43\text{ cm} \times 43\text{ cm}$ in less than 7 seconds with a compact laser-lens-CCD module. Details on performance (exposure sensitivity, effective spatial resolution, etc.) are not available, but a preliminary research paper describes some aspects of the system (Arakawa et al. 2004).

Another CR vendor is working on a similar system that uses an interesting “structured storage phosphor” that will purportedly combine good detection efficiency with good spatial resolution (characteristics that are usually trade-offs with unstructured phosphor materials). Even though information and details of these systems are somewhat sketchy, preliminary indications portend competitive capabilities and the use of CR technology and PSP detection/PSL conversion as viable alternatives to direct radiographic devices using 2-D CCD or flat-panel technology. Because of the compact size

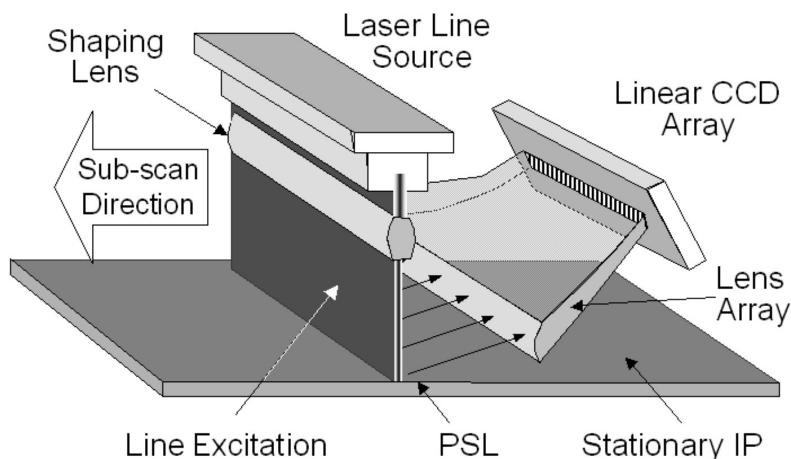


Figure 4. Component-level illustration of a line-scan CR detector. The laser source, shaping lens, PSL lens array, and CCD camera assembly move as a unit over the stationary imaging plate. Note that the lens array focuses the light emerging from the IP onto the corresponding detector elements of the CCD array. Not illustrated are individual lenses and color filters (to eliminate the stimulating laser signal) along the excitation array.

of the laser/detector module, the overall size of the detector has a similar form factor to that of a thin-film transistor direct radiography device, but currently at a much lower cost than a corresponding DR detector.

For the medical physicist, knowledge of the system capabilities and unique attributes compared to the conventional point-scan CR systems is important. Spatial and contrast resolution measurements, differences in row versus column resolution, overall dynamic range, typical detective quantum efficiency (DQE) capabilities, flatfield calibration techniques, etc., are necessary pieces of information to determine adequate system performance levels.

Image Data Pre-Processing

Shading Corrections

The “raw” data streaming from the CR reader requires shading corrections to compensate for variations in the light-guide response for a uniform exposure to the plate (Seibert 2003). For instance, equivalent PSL intensity captured at the edge of the light guide will have a lower response than if captured at the center of the light guide. Variations in the transmission efficiency will introduce static noise patterns that are reproduced at every scan. Over time, subtle deposits of material on the light guide produce fixed variations in light intensity. Adjustments to achieve uniformity are known as “shading corrections” applied to the raw data during acquisition. In the calibration mode, a uniformly irradiated IP of high-incident exposure (the latter to reduce quantum noise) is the source that measures the intensity gain response, G , at each position x along the scan, $G(x)$, averaged over n independent lines. The dark-level offset variations, O , are also measured at the same positions (x) along the scan, $O(x)$, and averaged over m independent lines, $O_m(x)$. The shading-normalized and averaged correction, $S(x)$, is calculated as

$$S(x) = \frac{M}{G_n(x) - O_m(x)}$$

where M is the global mean value of the evaluated profiles (the mean value of the denominator). Typically, $S(x)$ remains stable for a significant period (e.g., 6 months). As raw data are acquired, the dark current offset is subtracted from the incoming data at each scan position, x , and multiplied by the normalized shading correction array, producing the corrected data point, $I_C(x)$, as

$$I_C(x) = (I_{UC}(x) - O_m(x)) \times S_n(x)$$

1-D Shading Correction

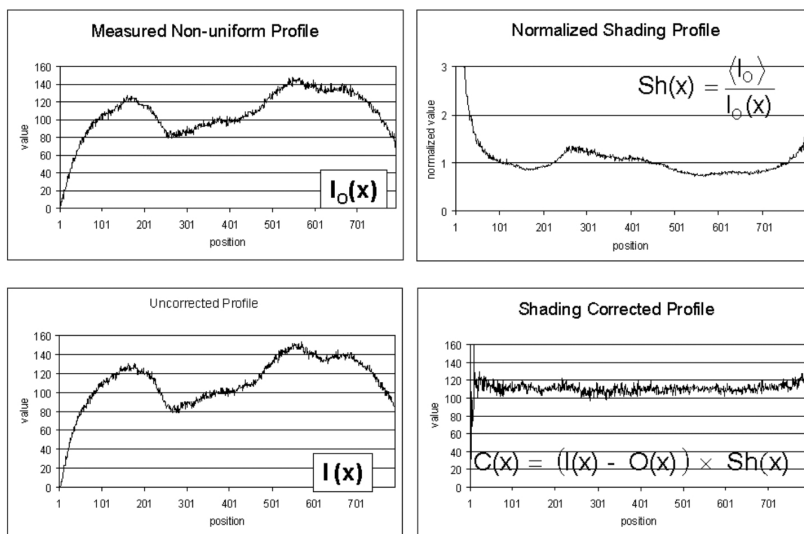


Figure 5. One-dimensional flatfield methods correct for “shading” variations caused by the repetitive variations in laser-beam output and light-guide pickup characteristics (Seibert 2003). This is not—and should not be—dependent on the emission characteristics of the IP and, in fact, requires an IP of uniform light output. [Reprinted from Seibert (2003) with permission from Radiological Society of North America (RSNA).

for all x positions along the fast-scan direction. These steps are illustrated for shading correction CR image in Figure 5. Because these are linear operations, this correction is performed prior to logarithmic or square-root transformation.

Newer line-scan systems can benefit from two-dimensional flatfield processing, which provides a more robust correction because of the reproducible scanning of the fixed detector. Two-dimensional corrections can improve the elimination of stationary noise patterns along the sub-scan direction not possible with point-scan systems that use imaging plates of different size and number.

Identification and Scaling of “Pertinent” Data

The raw digital image data must be properly identified prior to subsequent post-processing for specific anatomical display. This typically involves finding collimator borders for one or more exposures on the plate, specifically identifying the areas, and then producing a histogram from which the examination-specific distribution is used for determination of the minimum and maximum useful signals. Manufacturers employ different methods. A particularly straightforward and useful algorithm is a “shift and subtract”: the image is subtracted from an identical copy of itself and then

shifted in the horizontal and vertical directions by two or more pixels. This produces differential signals at locations of rapid change (e.g., collimator shadows) and identifies the area of interest. Algorithms to identify the resultant histogram shape—based upon the selected examination—are applied. Because the histogram distribution is strongly affected by anatomical variability, errors in shape identification occur as a result of collimator borders not correctly found, wrong examination, poor patient positioning, excessive scatter, highly attenuating objects such as prostheses, extreme under- or overexposure, and inappropriate kVp, among other causes. Failures were frequent with earlier systems. Although the potential problem list is long, advances in technology and algorithm improvements have reduced these errors to a small fraction. Figure 6 illustrates the data “finding” and “scaling” steps.

Compensation for under- and overexposure is a benefit of digital radiographic systems. This ability requires correct identification of the histogram shape, which is unchanged as long as the exposures fall within the dynamic range of the detector. Internal amplification (increased for underexposure and decreased for overexposure) results in a similar presentation of the output data that is independent of the incident exposure; however, image noise expressed as quantum mottle will be prevalent in the underexposed image, and image noise expressed as detector variations can be prevalent at very high exposures. In either case, patient care is compromised by the inability to achieve the optimal image and/or needless radiation overexposure to the patient. Variations in kVp will stretch or shrink a given histogram distribution, but smart algorithms are able to recognize this and compensate the latitude (slope) of the useful range. From a clinical perspective, the estimated exposure to the IP provides a feedback mechanism as a guide to assist in using proper radiographic techniques.

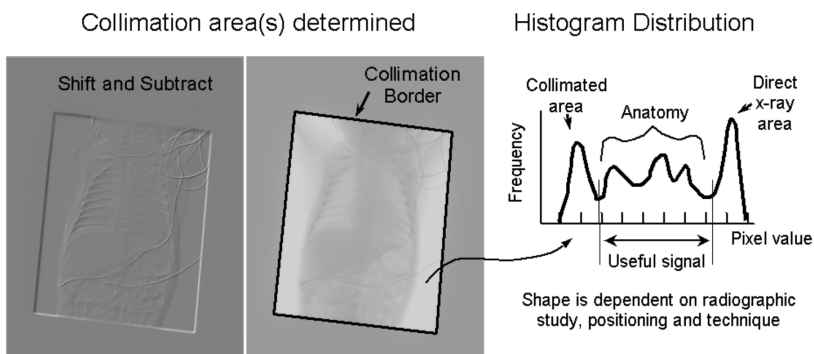


Figure 6. Shift and subtract reveals collimation borders and image area (left). Histogram analysis identifies minimum and maximum useful values within the defined collimation area to digitize over the range based upon the *anatomy-specific* shape (right). Incorrect histogram identification is often caused by positioning errors, collimator shadows off of the IP, or incorrect exam selection, among several causes.

Image Data Post-Processing

The “raw, scaled” CR data represents the baseline from which nonlinear contrast enhancement is applied. There are many contrast enhancement and spatial frequency algorithms, all of which strive to render the image with the anatomically best grayscale and detail. Image processing done poorly or inappropriately makes the image clinically inadequate. By the same token, excellent image processing cannot produce a clinically adequate image from poor pre-processing. Fortunately, reprocessing pre-scaled data and applying proper transformations can provide image quality good enough to reduce retakes to a minimum. Nevertheless, optimization of the processing algorithms according to radiologist preference during installation and at yearly intervals is extremely important.

Contrast Enhancement

The most simplistic contrast enhancement relies on non-linear transformation curves that mimic the response of a screen-film receptor. A variety of curves applied to the raw data provide wide latitude, high contrast, contrast inversion, etc. More sophisticated enhancement methods use a “harmonization” method, whereby a strongly blurred version of the image is weighted over a specific range of image values and subtracted from the original image. This approach will increase the apparent transmission under the diaphragm in a chest image by selectively reducing the slowly varying signal without affecting the detail and by reducing the dynamic range of the image. The overall contrast of the image can be increased simultaneously without saturation or thresholding of portions of the image. Dynamic Range Control is a common name for this particular type of image processing (Fuji 1993).

Spatial Frequency Enhancement

In addition to contrast enhancement, spatial frequency processing is also important in providing edge details for evaluation of bone trabeculae, pneumothorax, and other high-detail characteristics that are otherwise difficult to appreciate, particularly given the lower spatial frequency of CR compared to the conventional 400-speed screen-film combination. Spatial frequency enhancement can be applied in different ways as well. An easy method is the short-range blurring of an image—such as can be done with a 3×3 (or specifically designed) pixel “kernel” averaging of the original image—creating the blurred version from the central pixel values and taking the difference image. This results in a bandpass image that is scaled (depending on the degree of enhancement desired) and added back to the original image. The outcome is an edge-enhanced composite image, as shown in Figure 7.

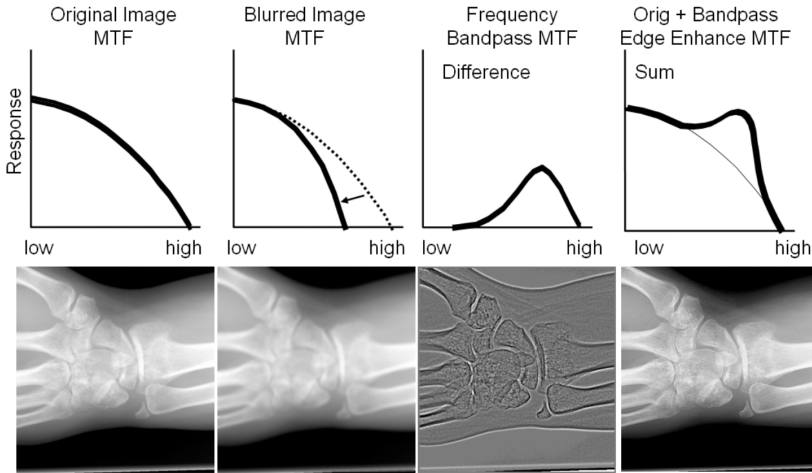


Figure 7. Simplified edge-enhancement example using a single bandpass frequency kernel is implemented by obtaining a blurred version of the image and subtracting from the original, giving a bandpass image with the bandpass frequency determined by the blurring kernel. A sum of the original image with the bandpass image results in the frequency-“boosted” image.

Multi-Scale, Multi-Frequency Enhancement

More sophisticated image processing methods use a “multi-scale” approach, whereby multiple scales (different bandpass ranges) of the same image are created by harmonization methods, from very low to very high frequency. Selective linear or non-linear amplification of each frequency band allows manipulation of the output image in terms of contrast enhancement, dynamic range control, and spatial frequency enhancement across all scales when combined to form the output image. Vendors have characteristic names for this type of image processing, including Multi-Scale Image Contrast Amplification (MUSICA) by Agfa (Vuylsteke and Shoeters 1994), Multi-objective Frequency Processing (MFP) by Fuji, and Enhanced Visualization Processing (EVP) by Kodak (VanMetter and Foos 1999). This type of processing is now becoming the standard mode of processing, chiefly because of the flexibility of the algorithm over multiple frequency ranges with the ability to achieve simultaneous increased contrast and selectable edge enhancement over all areas of the image. Figure 8 shows a simplified methodology of the multi-scale approach.

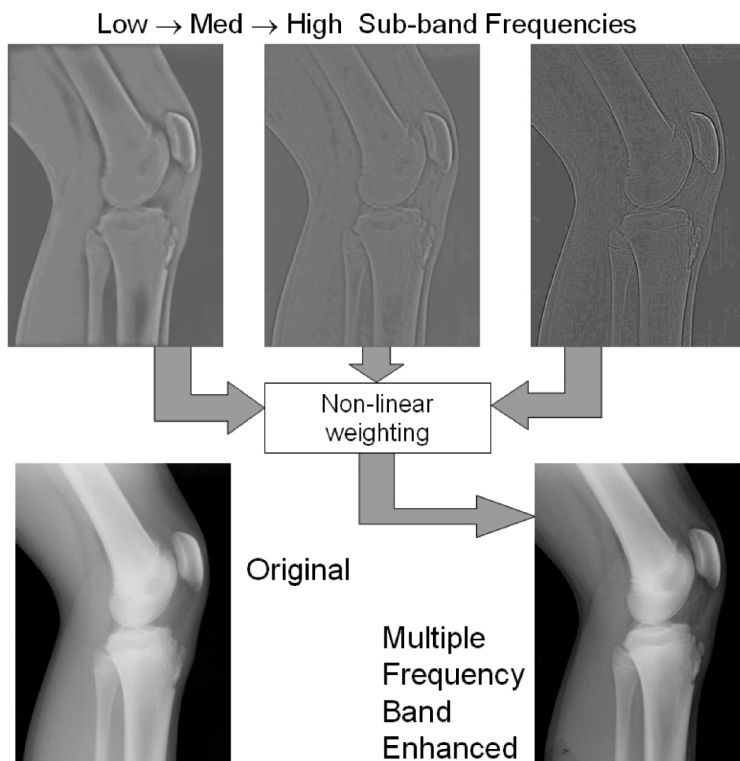


Figure 8. Multi-scale, multi-frequency approach for simultaneous contrast and frequency enhancement of images across all frequency ranges of the image. Typically, multiple frequency bands of eight or more are used; three are shown here. In this example, note the ability to enhance the soft tissue and bone contrast simultaneously compared to the original image.

Disease-Specific and Dual-Energy Processing with CR Imaging

Other advanced image processing techniques have “disease-specific” algorithms that emphasize characteristics that improve the detection of particular characteristics of the image based on the indication for the study or the suspected pathology, such as subtle linear structures to detect a pneumothorax (Siegel and Reiner 2001). Dual-energy radiography—made possible by the large dynamic range characteristics of CR detectors and the simultaneous acquisition of low- and high-energy images obtained with a copper filter sheet sandwiched between two IPs—provides the ability to generate tissue-selective images (bone and soft tissue—only renditions). Electronic imaging infrastructure combined with computer-aided diagnosis processing can bring sophis-

ticated detection capabilities to the general radiologist in the evaluation of pulmonary lesions and the ability to distinguish benign from malignant lesions (MacMahon 2000).

The Physicist's Role in CR Implementation

The physicist should be the technical expert and liaison between the radiology and hospital administrators, the radiologists, technologists, and IT/PACS staff. Knowledge of the CR system characteristics (resolution, detection efficiency, radiographic technique charts, sensitivity of the CR plate to scattered radiation and requirements for grids, compensation for under- and overexposure, decreased kV dependence, image processing, system specifications, etc.) is the key to being a successful arbitrator in a sometimes difficult—but necessary—transition from screen-film to CR/DR imaging. One critical role is the establishment of a training program that describes the changes in operation with CR. These changes include: exposure sensitivity of CR relative to that of 400-speed screen-film cassettes; the role of image processing in contrast optimization and noise suppression of the output radiograph (particularly for pediatric imaging); and how to implement and maintain ALARA (As Low As Reasonably Achievable) concepts using CR for this very radiosensitive population (Strauss 2004; Seibert 2004). Issues related to clinical considerations and details regarding exposure indicators as well as signal-to-noise ratio (SNR) and DQE details are described below. Acceptance testing and quality control tests are certainly part of the physicist's domain; these issues are covered in a separate article in these summer school proceedings.

Clinical Considerations

CR Reader Throughput

CR reader “stackers” versus single IP readers have a large impact on the throughput, chiefly because of the pipeline capabilities of reading and erasing IPs simultaneously. Also, an ability to insert multiple cassettes is a time-saver for the technologist, who can perform other tasks while the IPs are being processed. In a situation requiring the highest throughput, cassetteless CR systems can be employed that do not require handling after the exposure.

Phosphor Plates, Cassettes, Grids, Identification Terminals

Enough IPs of various sizes and corresponding cassettes should be ordered to meet 1.5 times the peak demand for imaging services. Low-frequency stationary grids (<100 lines/inch) can generate substantial moiré artifacts with digitally sampled images. High-frequency grids (e.g., >140 lines/inch or >55 lines/cm or higher, depending on the CR system) can alleviate problems with aliasing and moiré patterns and should be considered in conjunction with the CR purchase. Identification (ID) terminals provide

the patient demographic and modality worklist functionality that is critical for the elimination of PACS input errors and mislabeled images by correlating the exposed phosphor plate to the patient information (name, medical record number, etc.) and specific examination order (accession number). A sufficient number of ID terminals should be placed in convenient, strategic locations close to imaging areas to prevent bottleneck and throughput problems.

Incident Exposure Estimation and Other Data Fields

Incident exposure estimates for CR image acquisition are extremely important for tracking appropriate dose levels to patients and proper radiographic techniques by the technologist. They should be included as a requirement for monitoring and feedback purposes. In addition, a database of other performance indices should be considered, such as immediate warning of extremely high or low exposures, the number of times a phosphor plate has been put through the system (to track longevity), and processing parameters applied to the image, among other data fields.

Image-Processing Functionality

Specific image-processing capabilities should include simple window/level adjustments, non-linear adjustments to mimic screen-film response, reverse contrast mapping, edge enhancement, dynamic range compression, and dark-surround capability (to fill in the unexposed areas of the resultant image with dark or opaque boundaries—crucial for pediatric newborn studies and small objects). Image stitching and specialized cassettes for extended field-of-view (FOV) imaging capabilities are also important functions that should be evaluated. User-defined image processing capabilities are desirable.

CR Interfaces to RIS, HIS, Imaging Networks, and PACS

Interface of the CR system(s) to radiology and hospital information computers is extremely important. Details about the in-house RIS/HIS vendor must be explained. In return, the CR vendor should be expected to provide a standard interface [e.g., Health Level-7 (HL-7)], to achieve modality worklist functionality, which is essential in a PACS environment, and to provide automatic downloading/uploading of patient demographics, examination type, and scheduling times. A DICOM conformance statement for interface to existing or future PACS infrastructure, including network printers, is essential. All vendors typically have conformance statements posted on the World Wide Web for their particular equipment that list the capabilities and connectivity the systems can provide. This, however, is not a guarantee of DICOM connectivity or interoperability between the modality and the PACS or RIS because much functionality is optional and must be negotiated for or purchased at an added cost. The Integrating the

HealthCare Enterprise (IHE) provides a practical framework from which all of the actors generating and providing information can work together in a heterogeneous environment (RSNA 2004).

Quality Control Phantom Set and Software

The vendor should be requested to provide a quality control phantom and associated evaluation software with the system. This is often optional, but the physicist (or buyer) should insist on its purchase, possibly from a third-party vendor. Periodic measurement of spatial resolution, contrast resolution, exposure uniformity, exposure linearity, and distance measurement accuracy–aspect ratio should be available, along with software on the quality control workstation for automatic analysis.

Service Contracts, Preventive Maintenance, Warranty, and Siting Requirements

In addition to hardware and software maintenance/upgrades, IP longevity and warranty should be discussed. Approved third-party service or in-house radiological engineering support/training should be included as options. Siting requirements, required power, air-conditioning/filtering, equipment footprint, configuration of the CR readers, preliminary schematic drawings, etc., are all components of the specifications document for consideration.

Exposure Indicators

The wide latitude and signal-finding/scaling algorithms allow for a great flexibility in determining the amount of exposure desired for a given examination; however, potential problems with improper radiographic techniques and under- or overexposure can be masked. Underexposures yield very noisy images that are easily identified by the radiologist. More problematic is the overexposure, which most often yields excellent image quality, yet delivers too much dose to the patient without any increased information or benefit achieved from the diagnosis. Because of negative feedback due to underexposures, a predictable and unfortunate use of higher exposures, “dose creep,” is a typical occurrence (Seibert, Shelton, and Moore 1996). To identify an estimate of the exposure used for a given image, CR manufacturers have devised methods to analyze the digital numbers in the image based upon the calibrated response to known incident exposure.

Fuji CR: Sensitivity Number

Fuji CR systems use a sensitivity number, S , derived from the median value of the anatomy-specific histogram. In the case of underexposure, amplification of the signals

must be increased to map the median value to the mid value of the 10-bit output (code value = 511), and, in the case of an overexposure, amplification must be decreased. The degree of amplification provides an *estimate* of the incident exposure on the plate for the automatic and semiautomatic modes of operation. Under normal processing conditions, the system sensitivity number is given as (Fuji 1993)

$$S \cong \frac{200}{\text{exposure (mR)}}$$

When the system sensitivity number is equal to 200 with the “semiautomatic” or “automatic” readout mode, an average photostimulated luminescence within the area sensed by the CR reader can be *estimated* as 1 mR (80 kVp, no object, no added filtration other than inherent). If the histogram is inappropriately analyzed or the examination is changed, the S number will change and will possibly not be representative of the estimated incident exposure. For the *fixed* sensitivity mode available with the Fuji CR system, the sensitivity number is independent of the incident exposure on the plate and does not change with exposure (although the resultant image intensity and printed film does change, which makes the system’s performance similar to a screen-film detector).

Kodak CR: Exposure Index

Kodak CR systems use an exposure index, which is determined from the code values directly as an estimate of the incident exposure on the IP and is calculated as (Bogucki, Trauernicht, and Kocher 1995):

$$EI \cong 1000 \times \log(\text{exposure in mR}) + 2000$$

An exposure of 1 mR (80 kVp, 0.5 mm Cu, 1 mm Al filtration) will result in an exposure index of 2000. An exposure of 10 mR will result in an exposure index of 3000, and an exposure of 0.1 mR will result in a value of 1000 for general purpose (GP) IPs. High-resolution (HR) IPs are not quite as sensitive due to a thinner phosphor layer. The difference in the exposure index is the constant equal to 1700 instead of 2000, as indicated previously. Doubling the screen exposure will result in an increase of 300 in the exposure index value.

Agfa CR: IgM Database

Agfa CR systems utilize a relative exposure paradigm, which is available as an option to their systems (Agfa 2002; Samei et al. 2001). A calibrated dose value, called “IgM,” is the log of the median value of the histogram and is calculated for each scanned image associated with a given examination. After ~50 images of the same examination, the IgM mean value of “acceptable” exposures is stored as the reference value. Subsequent

image IgM values are compared to the reference value, and a graphical indicator is displayed in the text fields of each image. If a given exposure exceeds a predetermined threshold limit, a visible warning bar is printed and warning messages are logged into a database file. This procedure provides an exam-specific feedback indicator that allows the variable-speed characteristics of the CR system to be used to advantage.

CR Exposure Recommendations

Whichever exposure indicator method is used, the output values are sensitive to segmentation algorithms, effective energy of the beam (kVp, filtration), delay between exposure and readout, positioning of the patient relative to the phosphor, and the source-image distance, among other causes. Nevertheless, the exposure indicator number is important to quality assurance, patient exposure, and technologist training issues. In general, the optimal exposure required to provide good image quality at the lowest possible dose to the patient (Seibert 1996) for CR systems corresponds to an ~200 speed screen-film detector system, based upon the noise limitations of the image acquisition process. To use the CR system optimally, however, the incident exposures must be tuned to the specific examination. For example, tube placement exams that are frequently acquired to verify location can use significantly reduced exposures because of the relatively high signal of the tube. Likewise, for pediatric scoliosis exams, after the first “standard-dose” exam, repeat exams can be acquired at one-fourth the dose when the features of the vertebral column for measurement are needed (Strauss 2004). On the other hand, extremity exams requiring low noise and high detail should be acquired with a correspondingly higher dose. The bottom line is the need to tune the CR system exposure techniques to a level appropriate for each exam at acceptance testing and to continuously strive to ensure that these levels are consistently maintained through feedback and continuous training. Exposure indicators for CR should be audited at least quarterly and more frequently when first installing a unit. Guidelines for quality control of the exposure indicator are listed as a part of continuous quality control procedures in Seibert (2004) in this monograph.

Table 1 lists recommendations for exposure indices for given exams at UC Davis Medical Center, based upon operation of a Fuji 5000 CR unit for general adult imaging, which does not apply for pediatric or extremity imaging.

The incident dose required to achieve a given signal-to-noise ratio (SNR) for a CR detector is dependent upon many variables, including

1. X-ray absorption efficiency of the IP
2. Conversion efficiency of the PSP
3. Luminance variations of the PSL caused by phosphor variations
4. Light collection efficiency of the reader
5. Electronic noise during the readout
6. Detective Quantum Efficiency (DQE)

Table 1. Recommended “S” number limits for general “adult” imaging procedures. Values are based on a Fuji 5000 CR reader and “ST – V” imaging plates. Note: This does not apply to pediatric or extremity imaging, which will have slightly higher and slightly lower equivalent speed points, respectively. Assumed is proper positioning and exam processing algorithms matched to the anatomy imaged. Adapted from Willis (1996).

CR “S” number	Detector exposure (mR)	QC action to be taken
>1000	<0.2	Underexposed: REPEAT
600 – 1000	0.3 – 0.2	Underexposed: QC exception
300 – 600	1.0 – 0.3	Underexposed: QC review
150 – 300	1.3 – 1.0	Acceptable range
75 – 150	1.3 – 2.7	Overexposed: QC review
50 – 74	4.0 – 2.7	Overexposed: QC exception
<50	>4.0	Overexposed: QC REPEAT

With too low an incident exposure, the image is dominated by quantum statistics, the corresponding SNR is very poor, and the ability to detect subtle differences in x-ray attenuation is compromised. With too high an incident exposure, on the other hand, highly penetrated areas in the image will suffer from saturation effects and loss of contrast that cannot be adjusted. These recommendations depend on several issues, including the type of CR reader (newer systems, such as the dual-light collection systems, have a higher DQE and will consequently have a lower exposure recommendation for all indications), type of imaging plate (later-generation IPs have better exposure performance), quality of the CR reader and IP, and tolerance of the radiologist to image noise, among other considerations. Continuous analysis and feedback are required to get the optimal range of exposures and indications for a given examination at a given site.

Spatial Resolution, Contrast Resolution, and DQE

Spatial Resolution

High-contrast spatial resolution is determined by several factors that contribute to the modulation and loss of the signal, including (1) composition and thickness of the phosphor plate, (2) the size of the laser spot, (3) light scattering within the phosphor, and (4) PSL signal lag. Large x-ray absorption and high spatial resolution are usually not simultaneously achievable for producing the optimal image with CR (although some future photostimulable “structured” phosphors have been touted as being able to overcome this limitation). Typical CR phosphor thickness is on the order of 100 mg/cm² for BaFBr. A thicker phosphor layer absorbs more x-ray photons and produces more

trapped electrons in the matrix; however, PSL from the laser spot spreads out with depth, contributing to image blur. Digital image pixel size, usually between 100 and 200 μm , determines system spatial resolution at least up to the range of the effective blur diameter that is less than the pixel size. Digital sampling imposes a maximum frequency, the Nyquist frequency, equal to $(2\Delta x)^{-1}$ that can be accurately transferred through the system. Higher spatial frequencies contained in the spectrum beyond the Nyquist frequency will reflect back into the lower spatial frequencies and contaminate the image with “aliasing” artifacts such as moiré patterns. Unlike conventional screen-film detectors, smaller IPs will often provide better limiting resolution because the “effective” sampling pitch/aperture is determined by IP size (the number of samples is kept roughly constant, independent of the field of view). Spatial resolution is increased with a thinner phosphor layer, but the trade-off is lower detection efficiency and higher radiation dose. A majority of CR systems now use “standard” resolution IPs in lieu of the less dose-efficient “high-resolution” IPs. Phosphorescence lag and signal carry-over to adjacent pixels in the fast-scan direction cause the spatial resolution to be reduced near the Nyquist frequency.

Contrast Resolution

Contrast resolution depends upon several variables as well. The most important is the subject contrast generated by energy absorption differences of the tissues. In a digitally sampled system, the minimum difference between “noiseless” signals depends on the total number of possible digital values (quantization levels) as well as the target signal amplitude relative to the background. In most CR systems, digital values change with the logarithm or square root of the photostimulable luminescence, or equally with the logarithm radiation dose to the plate, so the numerical difference between digital values is the contrast. *Contrast sensitivity* of CR depends on the number of bits representing each pixel, on the gain of the system (e.g., number of electrons per x-ray photon or number of x-ray photons per analog-to-digital unit), and on overall noise amplitude relative to the contrast. The ability to differentiate a signal in the image of an object is strongly dependent on the inherent subject contrast (kVp and scatter acceptance), amount of noise (x-ray, luminance, electronic, and fixed pattern noise sources), image-viewing conditions, and the observer’s ability to discern regions of low contrast with respect to size. Digital post-processing can enhance contrast to a level limited only by the noise in the image. Noise sources contributing to the output image include the limited number of x-rays absorbed in the IP (quantum mottle), the stimulated luminescence variations during the readout process, quantization noise added by the analog-to-digital signal conversion (dependent upon the bit depth of the ADC, which is typically 10 to 12 bits in current systems), and electronic noise sources added during processing of the electronic latent image signals.

Detective Quantum Efficiency (DQE)

Detective Quantum Efficiency (DQE) is a measure of the signal transfer efficiency for a given incident exposure as a function of spatial frequency. DQE is determined on a system with a linear or linearizable system with respect to exposure variations. The characteristic curve response is used to linearize the system, and the presampled $MTF(f)$ and two-dimensional $NPS(f)$ values are measured to calculate the DQE as (Seibert Boone, and Cooper 2002; Samei and Flynn 2002)

$$DQE(f) = \frac{SNR_{out}^2}{SNR_{in}^2} = \frac{\langle PV \rangle^2 \times MTF(f)^2}{NPS(f) \times \phi} = \frac{NEQ(f)}{\phi}$$

In this equation, the SNR_{in}^2 is equal to the incident fluence (number of x-ray photons per unit area on the detector), and the SNR_{out}^2 is the square of the measured SNR of the output signal at a specific spatial frequency, f . This is determined by the measurement of the average global pixel value $\langle PV \rangle$, the $MTF(f)$, and the $NPS(f)$, as defined by specific methodologies (IEC 2003; AAPM 2004). NEQ is a measure of the “effective” noise characteristics of the detector as a function of spatial frequency. The $DQE(f)$ is measured over a range of incident exposures to determine incident exposure dependencies (if any) of the detector. Ideally, the DQE is 100% at all useful spatial frequencies, but in reality it is typically less than 30% for conventional CR detectors, mainly limited by the absorption efficiency of the phosphor. The DQE drops rapidly with spatial frequency because of a loss of signal modulation and a greater fraction of additive noise sources. As the incident exposure increases, a loss of DQE occurs at all spatial frequencies from an increase in noise contributions because of blemishes and thickness variations in the phosphor that are otherwise “hidden” by quantum noise at low incident exposures. DQE values indicate incident exposure requirements for a given SNR in the output image.

CR Manufacturers

Several manufacturers of CR equipment and major medical imaging companies cooperate with the original equipment manufacturers which design their own image-processing and data-handling algorithms. The reader is encouraged to search the Internet and other resources of medical imaging technology for vendor information and system specifications.

Conclusions

Computed radiography is now a mainstream technology that is quickly replacing screen-film technology for medical imaging, particularly as PACS and electronic medical record implementations continue to be vertically integrated over all sizes of

institutions and clinics. Knowledge of system operation from an imaging physics perspective is extremely important, particularly since the separation of the acquisition, display, and storage characteristics have eliminated the direct feedback of the screen-film technology that it replaces. Even though benefits are definitely gained with the implementation of CR, the cause-and-effect “disconnect” makes CR in some ways more difficult to use. In other ways, it leads to complacency and potential for radiation overexposure and thus requires continuous training and retraining to maintain optimal use of the equipment.

Regarding verification of optimal performance, the chapter entitled “Performance Testing of Digital Radiographic Systems: Part I” (Seibert 2004) in this monograph describes the recommended acceptance tests and a quality control program for CR systems.

References

- Agfa. (2002). Appendix C in Task Group #10 document. This and other Agfa literature available from Bayer Corporation, Agfa Division, Technical Imaging Systems, Ridgefield Park, NJ.
- American Association of Physicists in Medicine (AAPM). (2004). AAPM Task Group #20 on Noise Power Spectrum Methodology. Andrew Maidment, Chair.
- Arakawa, S., Y. Hiroaki, T. Kuwabara, H. Suzuki, T. Suzuki, and T. Hagiwara. (2004). “Compact high-speed computed radiography (CR) system using a linear CCD with a large-area photodiode (PD) and dual transfer lines.” *Proc SPIE* 5030:778–787.
- Bogucki, T. M., D. P. Trauernicht, and T. E. Kocher. “Characteristics of a Storage Phosphor System for Medical Imaging” in *Technical and Scientific Monograph No. 6*. Rochester, NY: Kodak Health Sciences Division, Eastman Kodak Company, 1995.
- Fuji Photo Film Co. Ltd.(Fuji). (1993). Automatic Setting Functions for Image Density and Range in the FCR System. Tokyo, Japan: Fuji Photo Film Co., Ltd., Computed Radiography, Technical Review No. 3.
- International Electrotechnical Commission (IEC). (2003). The International Electrotechnical Commission: Characteristics of digital x-ray imaging devices—Part 1: Determination of the detective quantum efficiency. IEC 62220-1. www.iec.ch.
- MacMahon, H. (2000). “Improvement in detection of pulmonary nodules: digital image processing and computer aided diagnosis.” *RadioGraphics* 20:1169–1177.
- Radiological Society of North America (RSNA). (2004). Integrating the Healthcare Enterprise. www.rsna.org/IHE/index.shtml.
- Samei, E., and M. J. Flynn. (2002). “An experimental comparison of detector performance for computed radiography systems.” *Med Phys* 29:447–459.
- Samei, E., J. A. Seibert, C. E. Willis, M. J. Flynn, E. Mah, and K. Junck. (2001). “Performance evaluation of computed radiography systems.” *Med Phys* 28(3):361–371.
- Seibert, J. A. “Performance Testing of Digital Radiographic Systems: Part I” in *Specifications, Performance Evaluation, and Quality Assurance of Radiographic and Fluoroscopic Systems in the Digital Era*. L. W. Goldman and M. V. Yester (eds.). AAPM 2004 Summer School Proceedings. Medical Physics Monograph No. 30. Madison, WI: Medical Physics Publishing, pp. 239–270, 2004.

- Seibert, J. A. "Image Quality and Dose." Presentation, ALARA in Pediatric Radiology Conference, Houston, TX, February 29. (To appear in an ALARA dose for digital radiography special edition of *J Pediatr Radiol* in 2004)
- Seibert, J. A. (2003) "Digital Radiographic Image Presentation: Preprocessing Methods" in Samei, E., and M. J. Flynn (eds.). *Advances in Digital Radiography: Categorical Course in Diagnostic Radiology Physics, 2003 Syllabus*. Radiological Society of North America, Inc., Oak Brook, IL, pp. 63–70, 2003.
- Seibert, J. A., J. M. Boone, and V. Cooper. (2002). "Quantitative analysis of a dedicated computed radiography system for mammography." *Proc SPIE* 4682:447–456.
- Seibert, J. A., D. K. Shelton, and E. H. Moore (1996). "Computed radiography x-ray exposure trends." *Acad Radiol* 3:313–318.
- Siegel, E., and B. Reiner. (2001). Presentation, Society of Computer Applications in Radiology (CARS 2001), Salt Lake City, UT, May 3–6, 2001.
- Strauss, K. (2004). "CR in Pediatric Imaging." Presentation, 8th Annual Digital X-ray and PACS Conference, St. Pete Beach, FL. Tarrytown, NY: AAF-MED (August A. Fink Memorial Education Division).
- Takahashi, K., K. Kohda, J. Miyahara, Y. Kanemitsu, K. Amitani, and S. Shionoya. (1984). "Mechanism of photostimulated luminescence in BaFX:Eu²⁺ (X=Cl, Br) phosphors." *J Lumin* 31/32:266–268.
- VanMetter, R., and D. H. Foos. (1999). "Enhanced latitude for projection radiography." *Proc SPIE* 3648:468.
- von Seggern, H., T. Voigt, W. Knupfer, and G. Lange. (1988). "Physical model of photostimulated luminescence of x-ray irradiated BaFBr:Eu²⁺." *J Appl Phys* 64(3):1405–1412.
- Vuytsteke, P., and E. Shoeters. (1994). "Multiscale image contrast amplification." *Proc SPIE* 2167:551–560.
- Willis, C. E. "Quality Improvement in Computed Radiography" in *Categorical Course in Physics: Technology Update and Quality Improvement of Diagnostic X-ray Imaging Equipment*, R. G. Gould and J. M. Boone (eds.). Oak Brook, IL: Radiological Society of North America Publication (RSNA), pp. 153–160, 1996.